

# polymer papers

## Photophysical and charge transfer studies of some model anthracene-backboned polyesters

K. R. Gorda\*, R. Varadaraj, D. G. Peiffer and C. Brons

Exxon Research and Engineering Company, Corporate Research, Route 22 East,  
Clinton Township, Annandale, New Jersey 08801, USA

(Received 8 November 1990; revised 13 May 1991; accepted 15 July 1991)

The preparation and characterization of several finely tailored anthracene-backboned polyesters are discussed. The anthracene fluorescence lifetimes ( $\tau$ ), fluorescence quenching kinetics ( $k_q$ ) and charge transfer equilibria ( $K_{ct}$ ) of the polymer-bound anthracene moieties (determined in chloroform) are also reported. Charge transfer complexation between the anthracene moiety and tetrachloro-1,4-benzoquinone (chloranil) is also investigated. In order to determine the extent of donor-acceptor equilibria,  $K_{ct}$  are determined from Benesi-Hildebrand plots. These results are correlated to the overall effects of the aliphatic bridging group, which appear to influence the micropolarity and vibrational and rotational properties of the anthracene moiety.

(Keywords: charge transfer complex; anthracene-backboned polyesters; fluorescence lifetime; charge transfer equilibrium; Benesi-Hildebrand plot)

### INTRODUCTION

The functionalization of polymers with electron-donating or electron-accepting groups (i.e. charge transfer) has led to some interesting discoveries. One striking feature, for example, is the dramatic enhancement in tensile modulus that often results when donor and acceptor polymers are blended<sup>1,2</sup>. These blends can also exhibit significant improvement in mechanical properties in comparison to the unblended components. These results are attributed to the 'crosslinking effect' incurred by the complexation of donor and acceptor functionality in the constituent polymer chains.

In addition, rheological studies of incompatible poly(butyl methacrylate) and poly(methyl methacrylate) blends have shown that the incorporation of donor and acceptor functionality into the methyl and butyl methacrylates, respectively, leads to an overall stabilization of the heterogeneous mixture<sup>3</sup>. Although this 'stabilized' blend is biphasic in nature, the  $T_g$  values of the donor and acceptor polymers are shifted when blended. In contrast, the  $T_g$  values of both components in the non-interacting (i.e. non-functionalized) blend show no change.

In summary, charge transfer interactions can have a significant effect on the mechanical and rheological properties of polymers. Although these effects are well documented<sup>4-6</sup>, little attention has been focused on understanding, at a molecular level, the structure-association relationships that exist between donor and acceptor polymers.

The present study deals with a spectroscopic investigation of a number of carefully tailored anthracene-backboned polyesters in solution. The anthracene group in the polymer backbone serves not only as an efficient electron-donating moiety in charge transfer complexation,

but also as an excellent spectroscopic probe to investigate polymer chain mobility and polymeric charge transfer behaviour in solution. Ultra-violet/visible absorption, steady-state fluorescence quenching and time-correlated photon-counting fluorescence lifetime techniques were employed. The results of this investigation are described in this paper.

### EXPERIMENTAL

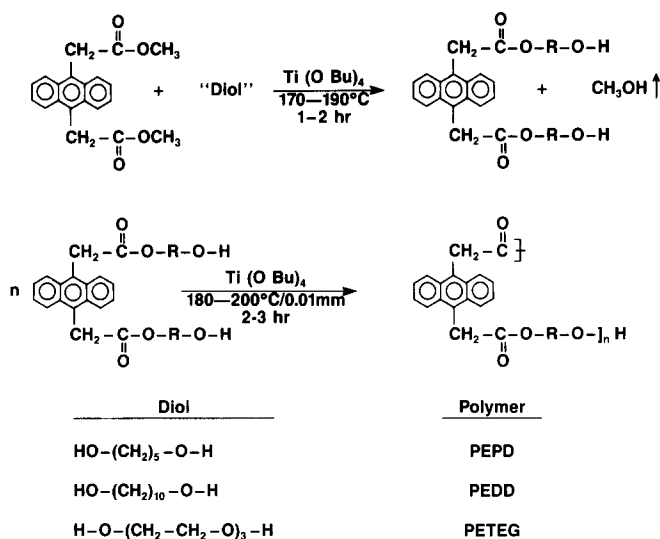
Anthracene (98%), paraformaldehyde (95%), hydrogen chloride gas (99%) and titanium(IV) n-butoxide were used as received (Aldrich). Triethylene glycol, 1,5-pentanediol and 1,10-decanediol were also used as received. Tetrachloro-1,4-benzoquinone (chloranil) (Aldrich) was recrystallized from toluene prior to use. The dimethyl ester of anthracene-9,10-diacetic acid was prepared according to a procedure described by Kretov<sup>7</sup> and Miller<sup>8</sup> and was recrystallized from methanol prior to use. Differential scanning calorimetry (d.s.c.) analysis was performed on a Perkin-Elmer DSC-2 at a heating rate of 10°C min<sup>-1</sup>. Reproducible  $T_g$  values were obtained in the second and third scans. Thermal gravimetric analysis was performed on a Perkin-Elmer TGA-2 with a heating rate of 20°C min<sup>-1</sup>.

#### Polymerization

Structural confirmation was performed by a variety of spectroscopic methods. I.r. spectra were recorded on a Perkin-Elmer 298 infrared spectrophotometer. <sup>1</sup>H n.m.r. spectra were obtained on a JEOL GX-400 and a Bruker EM-360. X-ray diffractometer scans were obtained using Cu K $\alpha$  radiation in order to observe crystallinity qualitatively.

The typical polymerization procedure is described in Scheme 1, where the polymer abbreviations are also given.

\* To whom correspondence should be addressed



Scheme 1

Approximately 3 g of diester and 10 g of diol were added to a 100 ml round-bottomed flask equipped with a magnetic stirrer. The mixture was placed under a nitrogen sweep and heated to 170°C, after which 2–3 drops of titanium(IV) *n*-butoxide were added. The monomers were then heated to approximately 190°C for 1–2 h. The vessel, after cooling, was quickly transferred to a vacuum line and maintained at 180–190°C (0.01 mmHg) for 2–3 h. The flask was cooled, removed from the vacuum line and the glassy solid was dissolved in approximately 80 ml chloroform. The solution was slowly added to a large excess of pentane to precipitate the polymer.

**PEDD.** I.r. (film from CHCl<sub>3</sub>): 1725 cm<sup>-1</sup> (ester carbonyl).

<sup>1</sup>H n.m.r. (CDCl<sub>3</sub>): 1.03 ppm (d, 12H), 1.43 ppm (s, 4H), 3.97 ppm (t, 4H), 4.52 ppm (s, 4H), 7.43 ppm (m, 4H), 8.23 ppm (m, 4H).

<sup>13</sup>C n.m.r. (CDCl<sub>3</sub>): 26.17, 28.92, 29.74 ppm (aliphatic methylene carbons), 34.22 ppm (-CHC<sub>2</sub>COO-), 65.56 ppm (-COOCH<sub>2</sub>-), 125.66, 126.61, 127.27, 130.85 ppm (aromatic), 171.76 ppm (carbonyl).

**PEPD.** I.r. (film from CHCl<sub>3</sub>): 1725 cm<sup>-1</sup> (ester carbonyl).

<sup>1</sup>H n.m.r. (CDCl<sub>3</sub>): 1.03 ppm (m, 2H), 1.35 ppm (m, 4H), 3.88 (t, 4H), 4.51 ppm (s, 4H), 7.44 ppm (m, 4H), 8.23 ppm (m, 4H).

<sup>13</sup>C n.m.r. (CDCl<sub>3</sub>): 22.25, 28.00 ppm (aliphatic methylene carbons), 34.52 ppm (-CH<sub>2</sub>COO-), 64.70 ppm (-COCH<sub>2</sub>-), 125.14, 125.74, 126.77, 130.33 ppm (aromatic), 171.18 ppm (carbonyl).

**PETEG.** I.r. (film from CHCl<sub>3</sub>): 1725 cm<sup>-1</sup> (ester carbonyl).

<sup>1</sup>H n.m.r. (CDCl<sub>3</sub>): 3.29 ppm (s, 4H), 3.56 ppm (s, 4H), 4.19 ppm (s, 4H), 4.61 ppm (s, 4H), 7.49 ppm (m, 4H), 8.27 ppm (m, 4H).

<sup>13</sup>C n.m.r. (CDCl<sub>3</sub>): 64.60, 69.32, 70.18 ppm (aliphatic methylene carbons), 34.53 (-CH<sub>2</sub>COO-), 125.53, 126.19, 127.10, 130.81 ppm (aromatic), 171.59 ppm (carbonyl).

### Fluorescence lifetime studies

Steady-state fluorescence spectra were recorded on a Perkin-Elmer model 650-40 spectrofluorimeter. Samples containing  $\sim 5 \times 10^{-4}$  M concentration in degassed chloroform were used. The excitation wavelength was 375 nm for all samples. Solution concentrations were adjusted so that all systems had the same number of absorbing species (anthracene) at 375 nm. This was achieved by adjusting the dilution in order that the optical density at 375 nm was the same for all systems.

Fluorescence lifetime ( $\tau$ ) was measured on the degassed samples ( $\sim 5 \times 10^{-4}$  M in chloroform) on a single-photon-counting PRA (System 3000) instrument. The excitation wavelength was 375 nm and monomer emission was monitored at 425 nm. Emission lifetime and pre-exponential factors were determined from the best fits to a bi-exponential decay using the non-linear least-squares deconvolution software provided by PRA. The analysis also provided estimates of the values of residuals, auto-correlation and reduced chi squared ( $\chi^2$ ).

The quenching rate constant ( $k_q$ ) was obtained from Stern-Volmer plots for  $5 \times 10^{-4}$  M anthracene fluorescence quenching by chloranil in chloroform at 25°C. The decrease in intensity of the 425 nm fluorescence peak as a function of quencher concentration was monitored. At this wavelength, neither chloranil nor the charge transfer complex exhibit any significant absorption.

### Charge transfer studies

The donor-acceptor equilibrium constants ( $K_{ct}$ ) of the anthracene-chloranil complex were measured in chloroform. U.v.-vis. absorption measurements were recorded using a Perkin-Elmer Lambda 7 Spectrophotometer using 1 cm quartz cells. The analysis consisted of the sample preparation of donor-acceptor solutions ( $\sim 4.26 \times 10^{-2}$  M donor,  $\sim 8.3 \times 10^{-3}$  M acceptor) with subsequent determination of the absorption maxima and optical density for the complex.

The spectra of pure monomer, polymer and chloranil do not show absorption to any significant degree in the region of the charge transfer band ( $\lambda \sim 660$  nm). Equilibrium constants ( $K_{ct}$ ) and molar extinction coefficients ( $\epsilon$ ) were calculated using a method originally described by Benesi and Hildebrand<sup>9</sup> employing a least-squares analysis.

For a 1:1 donor-acceptor complex, the equilibrium constant may be written as:

$$K_{ct} = [C]/[D][A] \quad (1)$$

where [C], [D] and [A] are the molar concentrations of complex, donor and acceptor, respectively. In sample preparation, [D] > [A] so [D] - [C]  $\approx$  [D]. The actual concentration of free acceptor is then [A] - [C]. The absorbance ( $d$ ) of the complex is related to its concentration by:

$$d = \epsilon l [C] \quad (2)$$

Substituting the absorbance terms in (2) into equation (1), the following expression can be obtained:

$$\frac{[A]l}{d} = \frac{1}{K_{ct}\epsilon[D]} + \frac{1}{\epsilon} \quad (3)$$

where  $l$  is optical path length (cm) and  $\epsilon$  is the molar extinction coefficient. The plot of [A]l/d vs. 1/[D] should be linear giving  $K_{ct}\epsilon$  as the reciprocal of the slope and  $\epsilon$  as the reciprocal of the  $y$  intercept.

RESULTS AND DISCUSSION

Anthracene-backboned polyesters were prepared by melt condensation polymerization of the dimethyl ester of anthracene-9,10-diacetic acid with the appropriate diol<sup>10</sup>. Typically high-molecular-weight polyesters of this type are poorly soluble in common organic solvents. Thus, in order to study the solution properties of these materials, polymerization methods were carefully controlled in order to obtain lower-molecular-weight polyesters that were soluble in chloroform. The i.r. and <sup>1</sup>H n.m.r. spectra (Figures 1 and 2) of the product polymers were used to determine their specific structure and are in accord with the exemplified structure shown in Scheme 1. A typical absorbance spectrum of the anthracene group is illustrated in Figure 3. The T<sub>g</sub> and thermal decomposition data are also included (Table 1).

These polymers are all bright yellow in colour, each possessing varying degrees of crystallinity depending upon the aliphatic sequence. Wide-angle X-ray scattering measurements reveal that the level of crystallinity is markedly enhanced by incorporating flexible or mobile segments (i.e. decamethylene) into the polymer. Moreover, it is anticipated that these aliphatic segments will affect the bulk solution properties via conformational changes within the polymer chain as reflected in their charge transfer and photophysical behaviour.

Excitation of anthracene at 375 nm in degassed chloroform (concentration of compound ~10<sup>-4</sup> M) results in emission at 406, 425 and 450 nm in all cases. Although emission wavelengths remain unchanged, the peak ratios (I<sub>2</sub>/I<sub>3</sub> and I<sub>2</sub>/I<sub>1</sub>) are different in all four cases (Figure 4). In general, the I<sub>2</sub>/I<sub>3</sub> and I<sub>2</sub>/I<sub>1</sub> values (Table 2) are observed to decrease upon incorporation of the anthracene moiety into the polymer backbone. Electronic transitions responsible for the I<sub>1</sub> and I<sub>3</sub> peaks are observed to be more favoured (or, conversely, I<sub>2</sub> less favoured) by fluorophore incorporation into the polymer backbone.

Fluorescence lifetime studies in fluorophores incorporated in polymer systems yield interesting information on the solution behaviour of the polymer itself. Most studies in this area have focused on the fluorophore being pendant to the polymer chain<sup>11</sup>. Fewer investigations, however, have been conducted on fluorophores incorporated into the polymer backbone. The present study provides examples of the latter case. Fluorescence

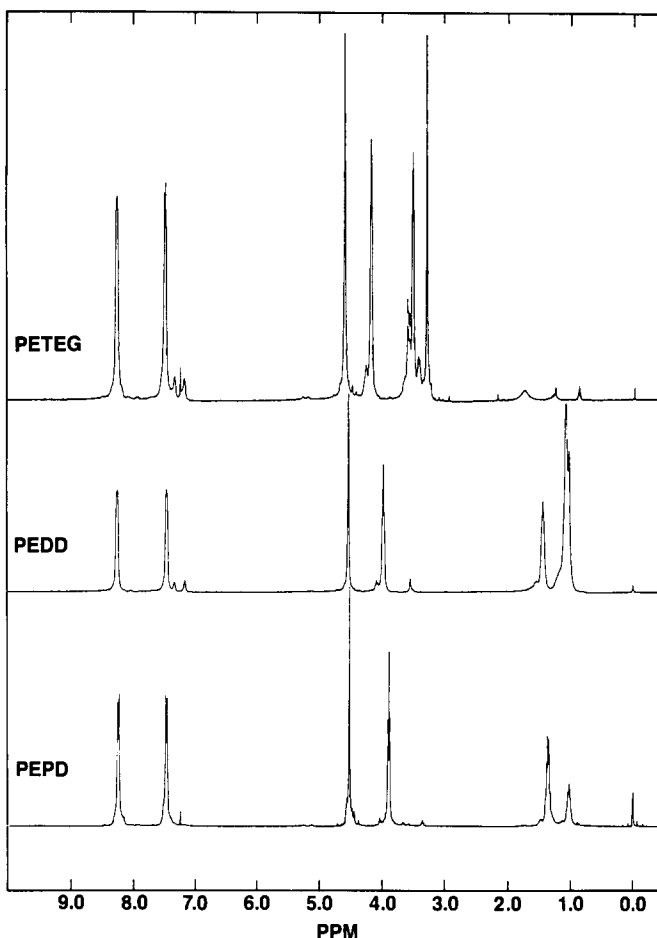


Figure 2 <sup>1</sup>H n.m.r. spectra of anthracene-backboned polyesters (CDCl<sub>3</sub> as solvent)

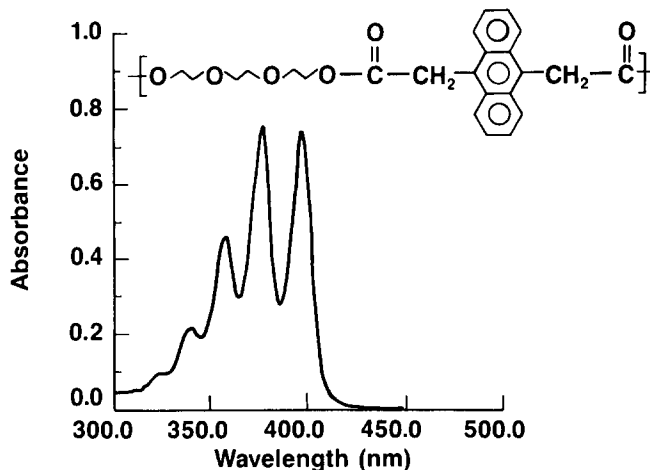


Figure 3 Typical absorbance spectrum of the anthracene moiety in the oxyethylene-bridged polyester (in chloroform)

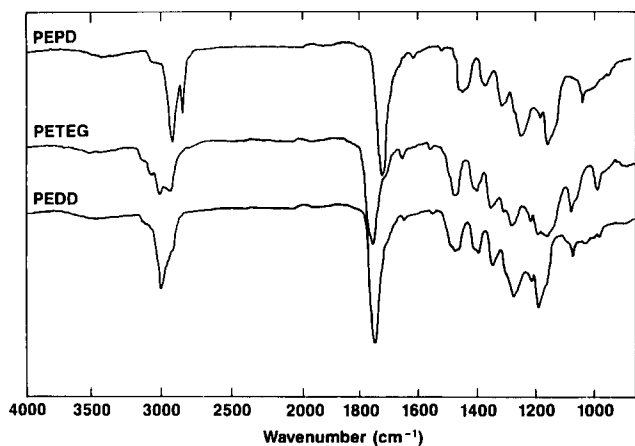


Figure 1 Infrared spectra of anthracene-backboned polyesters (film cast from chloroform)

Table 1 The T<sub>g</sub> and thermal decomposition data of donor polymers

Polymer	T <sub>g</sub> (°C)	Temperature (°C) for given weight loss <sup>a</sup>			
		25%	50%	75%	100%
PEDD	54	420	435	535	570
PEPD	61	395	420	535	555
PETEG	52	375	420	510	570

<sup>a</sup>In static air at temperature reported

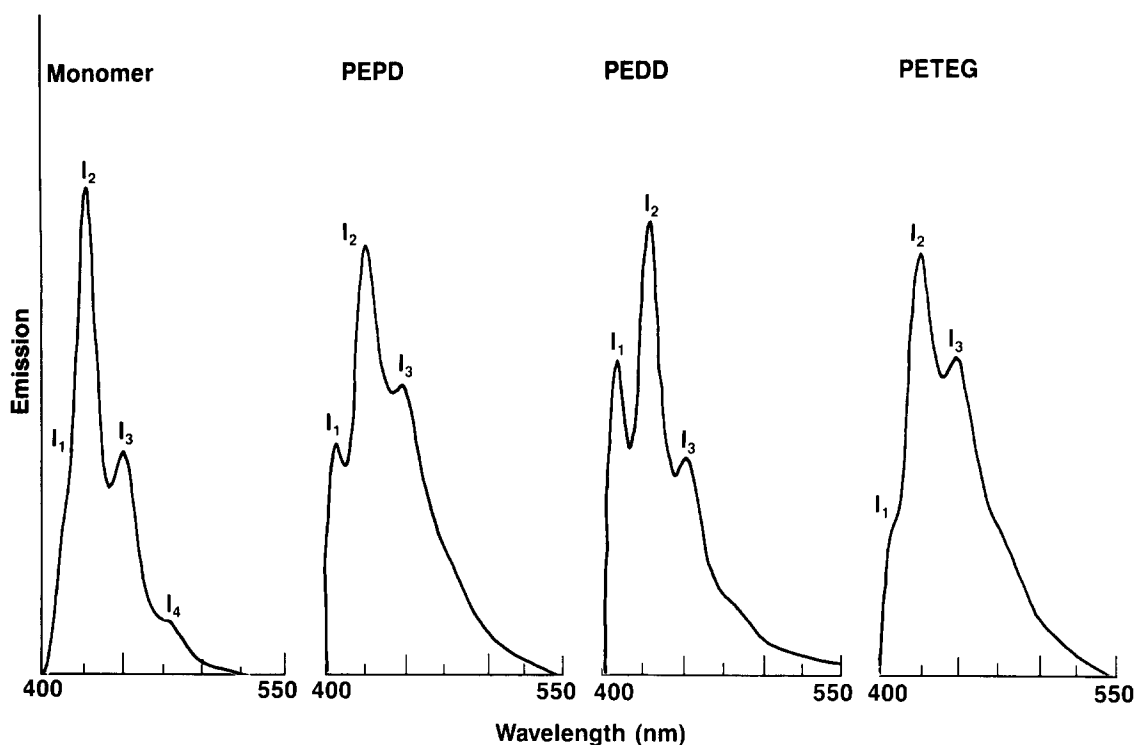


Figure 4 Emission spectra of polyester in chloroform (excitation wavelength 375 nm)

Table 2 Photophysical and charge transfer data of anthracene-backboned polyesters<sup>a</sup>

Compound	$I_2/I_1$	$I_2/I_3$	$\tau$ (ns)	$k_q$ ( $\text{mol}^{-1} \text{s}^{-1}$ )	$K_{ct}$ ( $\text{l mol}^{-1}$ )
Monomer	3.18	2.16	$16.9 \pm 0.4$	$29.44 \times 10^9$	1.31
PEPD	1.80	1.45	$16.7 \pm 0.9$	$28.87 \times 10^9$	1.19
PEDD	1.45	2.12	$14.9 \pm 0.9$	$34.37 \times 10^9$	1.27
PETEG	2.50	1.29	$27.4 \pm 1.7$	$22.0 \times 10^9$	1.12

<sup>a</sup> $\lambda_{ex}$  = 375 nm, solvent =  $\text{CHCl}_3$  (anthracene)  $\sim 10^{-4}$  M,  $T = 25^\circ\text{C}$   
 Emission bands:  $I_1 = 406$  nm,  $I_2 = 425$  nm,  $I_3 = 450$  nm  
 Fluorescence quenching: 425 nm emission band monitored ( $\lambda_{ex}$  = 375 nm)  
 $K_{ct}$ :  $\lambda_{max} \approx 660$  nm,  $[D] = 3 \times 10^{-2}$  to  $25 \times 10^{-2}$  M,  $[A] = 8.13 \times 10^{-3}$  to  $9.10 \times 10^{-3}$  M

lifetimes ( $\tau$ ) of the anthracene moiety in each of the polymers are reported in Table 2. Best fits of the decay curve (Figure 5) were obtained by a bi-exponential fit. The shortest-lifetime component with the largest amplitude factor (>99%) was observed to be  $\sim 16$  ns, for monomer, PEPD and PEDD. However, for PETEG, the value of  $\tau$  was 27 ns. This suggests that the rotational deactivation of the excited anthracene is sluggish in PETEG in comparison to the others. The conformation, rigidity and polarity of the oxyethylene sequence may be influential on the rotational motion of the polymer-bound anthracene. The fluorescence lifetime data suggest that the dynamics of the oxyethylene-bridged polymer (in solution) is quite different from that of the methylene-bridged counterparts.

Results obtained from the fluorescence lifetime experiments prompted a study of the fluorescence quenching of anthracene by chloranil. The objective was to investigate whether the nature of the bridging group between the anthracene moieties had any influence on the kinetics of the anthracene interaction with a quenching molecule.

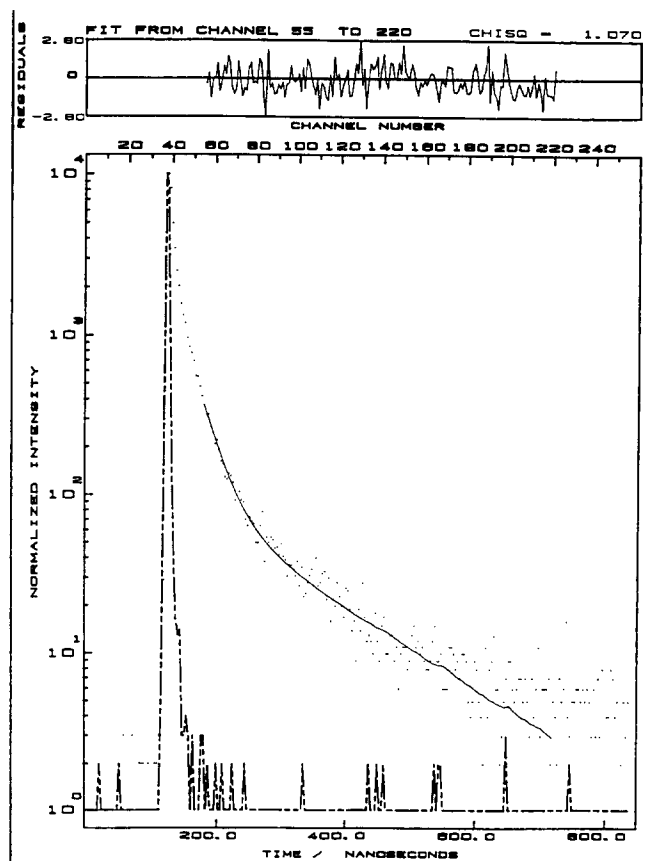


Figure 5 Typical fluorescence decay curve of the anthracene moiety in the oxyethylene-bridged polyester in chloroform

Rate constants  $k_q$  for the quenching of anthracene ( $\sim 10^{-4}$  M in chloroform) in these systems were studied using chloranil as quencher and obtained from Stern–Volmer plots. The slope of the plot  $I_0/I$  versus quencher concentration generated  $k_q\tau$  values. Using the value of  $\tau$

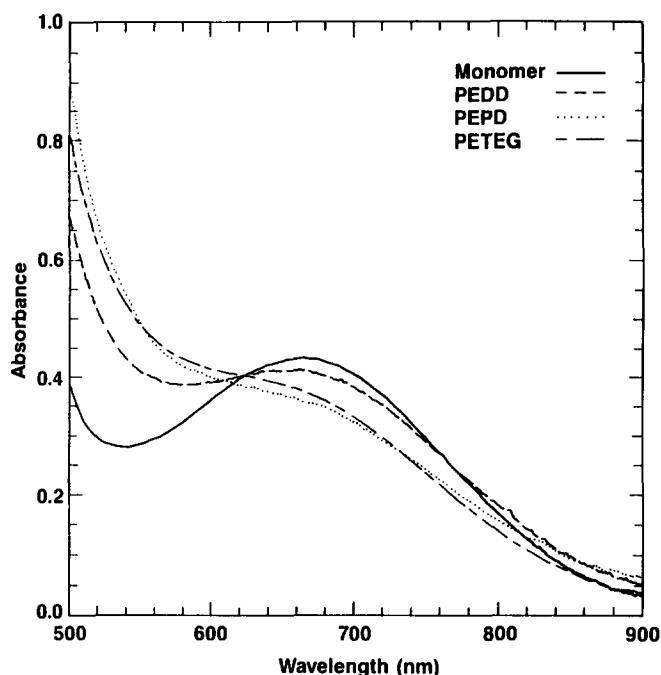


Figure 6 Absorption spectra of model donor-chloranil complexes in chloroform;  $[D] = (4.1-6.2) \times 10^{-2} \text{ M}$ ,  $[A] = (8.3-9) \times 10^{-3} \text{ M}$

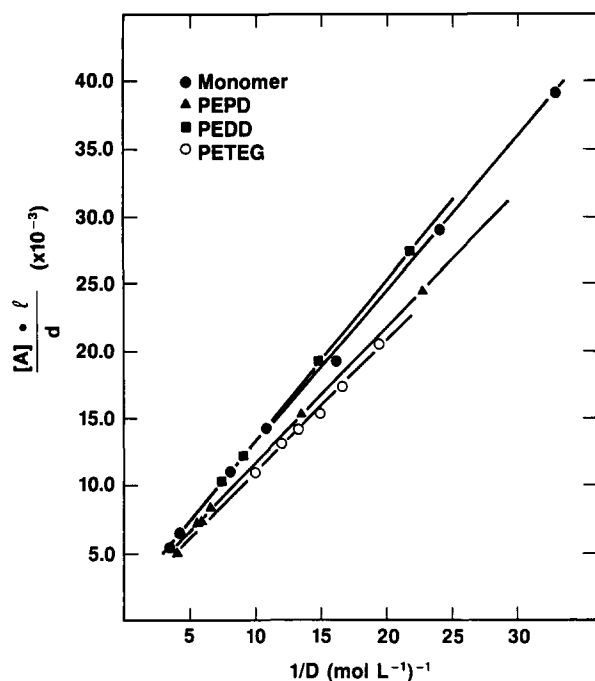


Figure 7 Benesi-Hildebrand plots of polyester-chloranil complexes in chloroform

from the fluorescence lifetime experiments,  $k_q$  was calculated. An interesting relationship between  $k_q$  and the nature of the bridging group is observed. When the number of methylene units spacing anthracene is increased from 5 to 10,  $k_q$  increases from  $28.8 \times 10^9 \text{ mol}^{-1} \text{ s}^{-1}$  to  $34.3 \times 10^9 \text{ mol}^{-1} \text{ s}^{-1}$ . However, introduction of the oxyethylene bridge between anthracene groups reduces the rate constant for quenching to  $22.0 \times 10^9 \text{ mol}^{-1} \text{ s}^{-1}$ . The sensitivity of  $k_q$  to the aliphatic segment of these polyesters suggests that the kinetics of interaction between the anthracene group and chloranil (in solution)

is affected by the nature of the bridging group between the anthracene functionalities.

Charge transfer complexes of these polyesters with tetrachloro-1,4-benzoquinone (chloranil) were examined. Results were compared to those obtained using the monomeric diester as electron donor in order to ascertain the effect of the polymer chain on complexation behaviour.

Shown in Figure 6 are the absorption spectra of monomer and polymer complexes with chloranil. Monomer and PEDD complexes possess an absorption maximum at 662 nm. Absorption maxima are not detected for the complexes involving the PEPD and PETEG polyesters. A result common to all three donor polymers, however, is the apparent increase in absorption at lower wavelengths. In order to determine quantitatively the extent of these interactions, Benesi-Hildebrand plots were constructed from the optical data. A typical Benesi-Hildebrand plot of the diester-chloranil complex is exemplified in Figure 7. From these plots, equilibrium constants ( $K_{ct}$ ) and molar extinction coefficients ( $\epsilon$ ) were calculated from reciprocal slope and intercept data and are also summarized in Table 2. A comparison of the  $K_{ct}$  values for these complexes does reveal that donor-acceptor interactions are comparable.

## CONCLUSION

In summary, these results have shown that, in this series of finely tailored anthracene-backboned polyesters, macromolecular effects induced by the polymer chain influence the electronic, photophysical and associative properties of the polymer-bound anthracene moiety as measured by anthracene fluorescence lifetimes, quenching, kinetics and complexation behaviour. For example, the impact of the bridging group on the electronic properties of anthracene is reflected in the differences in the peak ratios in the emission spectra of these materials as well as differences found in their fluorescence lifetimes. In general, the electronic transitions responsible for  $I_1$  and  $I_3$  peaks appear to be favoured by the incorporation of the anthracene group into the polymer backbone. While differences in the fluorescence lifetimes of these materials (i.e. monomer and pentamethylene- and decamethylene-bridged polymers) appear modest, the effect of the oxyethylene segment noticeably increases the fluorescence lifetime of the anthracene group in that polymer.

The photophysical properties of the polymer-bound anthracene moiety appear affected by the following: (i) polarity of the polymer coil in which they reside; (ii) rigidity of the polymer backbone, which influences rotational motion of the anthracene group.

The observed correlation between the methylene/oxygen ratio and the photophysical properties  $I_2/I_1$ ,  $I_2/I_3$ ,  $\tau$ ,  $K_q$  and  $K_{ct}$  (Table 2) suggests that the micropolarity around the anthracene moiety affects these properties. As the methylene/oxygen ratio decreases, the polarity of the anthracene micro-environment is increased. Thus PETEG provides the most polar environment and PEDD the least.

In addition to increasing the micropolarity around the polymer chain, the oxyethylene bridging may also be restricting free rotation of the anthracene group by inducing the polymer chain to adopt a particular conformation, thereby reducing overall chain flexibility. The combined influence of increased micropolarity and

restricted motion explains the observed photophysical properties in PETEG, PEDD and PEPD polyesters.

In conclusion, the photophysical and charge transfer studies performed on these specifically tailored anthracene-backboned polyesters have provided useful insight into the associative and structure–property relationships of these materials.

## REFERENCES

- 1 Sulzberg, T. and Cotter, R. *J. Polym. Sci., Polym. Chem. Edn.* 1969, **2**, 146
- 2 Sulzberg, T. and Cotter, R. *J. Polym. Sci., Polym. Chem. Edn.* 1970, **8**, 2747
- 3 Schneider, H. S., Cantow, H., Lutz, R. and Neto, H. N. *Makromol. Chem., Suppl.* 1984, **8**, 89
- 4 Simionescu, C., Onofrei, G. and Grigoras, M. *Makromol. Chem., Rapid Commun.* 1984, **5**, 229
- 5 Tazuke, S., Nagahara, H. and Matsuyama, Y. *Makromol. Chem.* 1980, **181**, 2199
- 6 Matsuyama, Y. and Tazuke, S. *Makromol. Chem.* 1975, **176**, 1657
- 7 Kretov, A. and Litinov, V. V. *Zh. Prikl. Khim.* 1962, **35**, 464
- 8 Miller, M., Amidon, R. and Tawney, P. O. *J. Am. Chem. Soc.* 1955, **77**, 2845
- 9 Benesi, H. A. and Hildebrand, J. H. *J. Am. Chem. Soc.* 1949, **91**, 2703
- 10 Gorda, K. R., Peiffer, D. G. and Denney, D. B. *J. Polym. Sci., Polym. Chem. Edn.* 1990, **28**, 3513
- 11 Tazuke, S. and Banba, F. *J. Polym. Sci., Polym. Chem. Edn.* 1976, **14**, 2463